Experimental Physiology

Characterization of the slowly inactivating sodium current I_{Na2} in canine cardiac single Purkinje cells

L. Bocchi and M. Vassalle

Department of Physiology and Pharmacology, State University of New York, Downstate Medical Centre, 450 Clarkson Avenue, Brooklyn, NY 11203, USA

The aim of our experiments was to investigate by means of a whole cell patch-clamp technique the characteristics of the slowly inactivating sodium current (I_{Na2}) found in the plateau range in canine cardiac Purkinje single cells. The I_{Na2} was separated from the fast-activating and -inactivating I_{Na} (labelled here I_{Na1}) by applying a two-step protocol. The first step, from a holding potential (V_h) of −90 or −80 mV to −50 mV, led to the quick activation and inactivation of I_{Na1}. The second step consisted of depolarizations of increasing amplitude from −50 mV to less negative values, which led to the quick activation and slow inactivation of I_{Na2}. The I_{Na2} was fitted with a double exponential function with time constants of tens and hundreds milliseconds, respectively. After the activation and inactivation of I_{Na1} at −50 mV, the slope conductance was very small and did not change with time. Instead, during I_{Na2}, the slope conductance was larger and decreased as a function of time. Progressively longer conditioning steps at −50 mV resulted in a progressive decrease in amplitude of I_{Na2} during the subsequent test steps. Gradually longer hyperpolarizing steps (increments of 100 ms up to 600 ms) from V_h −30 mV to −100 mV were followed on return to −30 mV by a progressively larger I_{Na2}, as were gradually more negative 500 ms steps from V_h −30 mV to −90 mV. At the end of a ramp to −20 mV, a sudden repolarization to approximately −35 mV fully deactivated I_{Na2}. The I_{Na2} was markedly reduced by lignocaine (lidocaine) and by low extracellular [Na^+], but it was little affected by low and high extracellular [Ca^{2+}]. At negative potentials, the results indicate that there was little overlap between I_{Na2} and the transient outward current, I_{to}, as well as the calcium current, I_{Ca}. In the absence of I_{to} and I_{Ca} (blocked by means of 4-aminopyridine and nickel, respectively), I_{Na2} reversed at 60 mV. In conclusion, I_{Na2} is a sodium current that can be initiated after the inactivation of I_{Na1} and has characteristics that are quite distinct from those of I_{Na1}. The results have a bearing on the mechanisms underlying the long plateau of Purkinje cell action potential and its modifications in different physiological and pathological conditions.

(Received 2 October 2007; accepted after revision 2 November 2007; first published online 9 November 2007)
Corresponding author M. Vassalle: Department of Physiology, Box 31, SUNY, Downstate Medical Center, 450 Clarkson Avenue, Brooklyn, NY 11203, USA. Email: mario.vassalle@downstate.edu

In canine heart, the plateau of the action potential (AP) of Purkinje fibres is much longer than that of myocardial ventricular myocytes (529.7 *versus* 310.1 ms, Lin & Vassalle, 1978). The fact that the Purkinje fibre plateau is markedly shortened by tetrodotoxin (TTX; Coraboeuf *et al.* 1979; Bhattacharyya & Vassalle, 1982) and by local anaesthetics (Weidmann, 1955; Vassalle & Bhattacharyya, 1980; Carmeliet & Saikawa, 1982), whereas it is prolonged by high extracellular [Na^+] ([Na^+]$_o$) and veratridine (Iacono & Vassalle, 1990) suggests the presence a slowly inactivating sodium current.

In cardiac tissues, several TTX-sensitive late sodium currents have been reported, namely: (i) the background sodium current (Coraboeuf *et al.* 1979; Zilberter *et al.* 1994); (ii) the window current (Attwell *et al.* 1979); (iii) a persistent sodium current found in ventricular myocytes (Saint *et al.* 1992; Zygmunt *et al.* 2001; Noble & Noble, 2006; Belardinelli *et al.* 2006); and (iv) a slowly inactivating current in canine (Gintant *et al.* 1984) and rabbit Purkinje fibres (Carmeliet, 1987).

In this context, it should be underlined that the AP duration of ventricular myocytes is very little affected by

 DOI: 10.1113/expphysiol.2007.040881

TTX (Coraboeuf *et al.* 1979; Bhattacharyya & Vassalle, 1982), by local anaesthetics (Vassalle & Bhattacharyya, 1980) and by veratridine (Iacono & Vassalle, 1990), suggesting that the findings in Purkinje fibres cannot *ipso facto* be extended to ventricular myocytes and vice versa (see also Discussion).

The current contributing to the long plateau has been studied in single Purkinje cells. During 500 ms voltage clamp steps from a holding potential (V_h) of −80 mV to −50 mV, the fast sodium current (I_{Na}; here designated I_{Na1}) activated and inactivated quickly; during the remainder of the step the current did not vary as a function of time. With depolarizing steps to −40 mV or to less negative values, I_{Na1} activated and inactivated quickly as usual, but the final phase of I_{Na1} inactivation was overlapped by a slowly decaying inward component (designated I_{Na2}), whose inactivation was not complete even by the end of the step. Both I_{Na1} and I_{Na2} were decreased by a less negative V_h and by TTX (Vassalle *et al.* 2007).

These findings suggested that I_{Na1} and I_{Na2} have different characteristics, but the overlap of the activation and inactivation of these two currents hindered the further analysis of I_{Na2}. Therefore, the general aim of the present experiments was to separate I_{Na2} from I_{Na1} and then investigate some of its properties. The specific aims were to determine the following characteristics of I_{Na2}: (i) activation separated from that of I_{Na1}; (ii) kinetics of activation *versus* inactivation; (iii) changes in slope conductance; (iv) time-dependent inactivation; (v) time- and voltage-dependent recovery from inactivation; (vi) deactivation on repolarization; (vii) dependence on $[Na^+]_o$; (viii) overlap with the transient outward current, I_{to}; (ix) possible contribution of calcium current, I_{Ca}, to the slowly decaying inward component; and (x) the reversal potential of I_{Na2} in the presence of block of I_{to} and of I_{Ca}.

The use of the patch-clamp technique in single Purkinje cells avoided the complication related to accumulation/depletion of ions in narrow extracellular spaces occurring in non-dissociated Purkinje strands (Baumgarten & Isenberg, 1977; Cohen & Kline, 1982) and permitted a better voltage control.

The results obtained indicate that I_{Na2} can be separated from I_{Na1} and that it is a rapidly activating, slowly inactivating sodium current with a threshold, voltage range, magnitude and inactivation–reactivation kinetics which are distinctly different from those of I_{Na1} as well as of other persistent sodium currents described in myocardial tissue. Because of its characteristics, I_{Na2} may regulate the plateau duration of Purkinje fibres in a number of physiological and pathological conditions independently of regulation of the upstroke by I_{Na1}.

Methods

The experiments were performed in accordance with national and institutional ethical guidelines. The protocols for the experiments were reviewed and approved by the local Animal Care and Use Committee.

The details of the methods have been recently published (Vassalle *et al.* 2007). In brief outline, 25 adult dogs (beagle) of either sex, weighing 9–14 kg, were killed by intravenous injection of sodium pentobarbitone (60 mg kg^{-1}). Once respiration had stopped, the hearts were removed and rinsed in Tyrode solution. Purkinje fibre bundles were dissected out from both ventricles and were driven at 60 min^{-1} for 30 min while being superfused in the tissue bath at 37°C.

The composition of the Tyrode solution (mM) was: NaCl, 140; KCl, 5.4; $CaCl_2$, 1.8; $MgCl_2$, 1; Hepes, 5.0; and glucose, 5.5. The solution was gassed with 100% O_2 and adjusted at pH 7.4 with NaOH. The fibres were then rinsed with Ca^{2+}-free solution for 5 min in the same tissue bath and washed in a test tube three times with the same Ca^{2+}-free solution. The Ca^{2+}-free solution contained (mM): NaCl, 140; KCl, 5.4; KH_2PO_4, 1.2; $MgCl_2$, 1.5; Hepes, 5.0; and glucose, 5.5 (pH adjusted to 7.2 with NaOH).

Purkinje strands were digested at 37.5°C in the Ca^{2+}-free Tyrode solution to which collagenase, elastase and essentially fat-free bovine serum albumin had been added ('enzyme solution'). The digested fibres were separated by agitation by means of a mechanical 'triturator' (Datyner *et al.* 1985). The cells were suspended in a Kraftbrühe (KB) solution, and a sample of the cell suspension was superfused with Tyrode solution at 37°C in a chamber located on the stage of an inverted microscope (Nikon Diaphot).

We employed the whole cell patch-clamp technique using an Axopatch 1D amplifier. The pipettes were filled with the following solution (mM): potassium aspartate, 100; KCl, 30; $MgCl_2$, 2.0; EGTA, 11.0; sodium Hepes, 10.0; Na_2-ATP, 2.0; NaGTP, 0.1; and $CaCl_2$, 5.0 (pH 7.2; resistance 2–4 MΩ). The free $[Ca^{2+}]$ in the pipette solution was 110 nM as calculated using a computer program (Winmaxc 2.40; available at http://stanford.edu/~cpatton/maxc.html). The electrical signals were digitized at 333 kHz 12-bit resolution using an A/D converter (Digidata 1200, Axon Instruments Inc., Sunnyvale, CA, USA) and recorded using Clampex software (pCLAMP 8.0, Axon Instruments) and low-pass filtering at 2 kHz.

The Purkinje cells were studied under control conditions in the absence of any channel blocker (such as Ba^{2+}, Cs^+, Ni^{2+}, lignocaine or 4-aminopyridine) to explore the behaviour of the currents under physiological conditions. Only after the control recordings had been carried out were some of these blockers tested to investigate at which potentials other currents overlapped

I_{Na2}. Successive command steps of the same protocol were applied at intervals of at least 5 s, and different protocols were separated by intervals of 3–5 min to allow the effects of each procedure to fully subside. If the patch-clamp recording became unstable with time, the procedures were discontinued.

Data were analysed by means of the pCLAMP program (Axon Instruments). Steps from different values of V_h were applied to activate voltage- and time-dependent currents and ramps to elicit I_{Na2} in the presence and absence of I_{Na1}. On step depolarizations from the resting potential, I_{Na1} was often cut off at −10 nA by saturation of the amplifier.

The amplitude of the slowly decaying inward component of I_{Na2} was measured as the difference between the current at the beginning and the end of the step. The beginning was taken as the value at the intersection between the rapidly inactivating I_{Na1} and the backward extrapolation of I_{Na2}, also checked with the fitting of slowly inactivating I_{Na2} with a double exponential function.

The inactivating I_{Na2} traces were fitted with a two-term standard exponential function using the Chebyshev technique with Clampfit software according to eqn (1):

$$I(t) = A_1 \exp(-t/\tau_1) + A_2 \exp(-t/\tau_2) + C \quad (1)$$

where A_1 and A_2 are the amplitudes, τ_1 and τ_2 are the time constants, and C is the offset constant. Data were analysed by mean of the Clampfit (pCLAMP 8.0) and Microsoft Excel programs. Results of the tests carried out (n) are shown as means ± S.E.M. Student's paired t test between two terms of comparison and one-way ANOVA between a data group were applied and $P < 0.05$ was considered significant.

Results

I_{Na2} after the separation from I_{Na1}

A double depolarizing step was applied as illustrated by the protocol in inset *a* in Fig. 1*A*. After the inactivation of I_{Na1}, during the second step at −60 or −50 mV, no time-dependent current was present. During the step to −40 mV, a fast small inward transient appeared (first

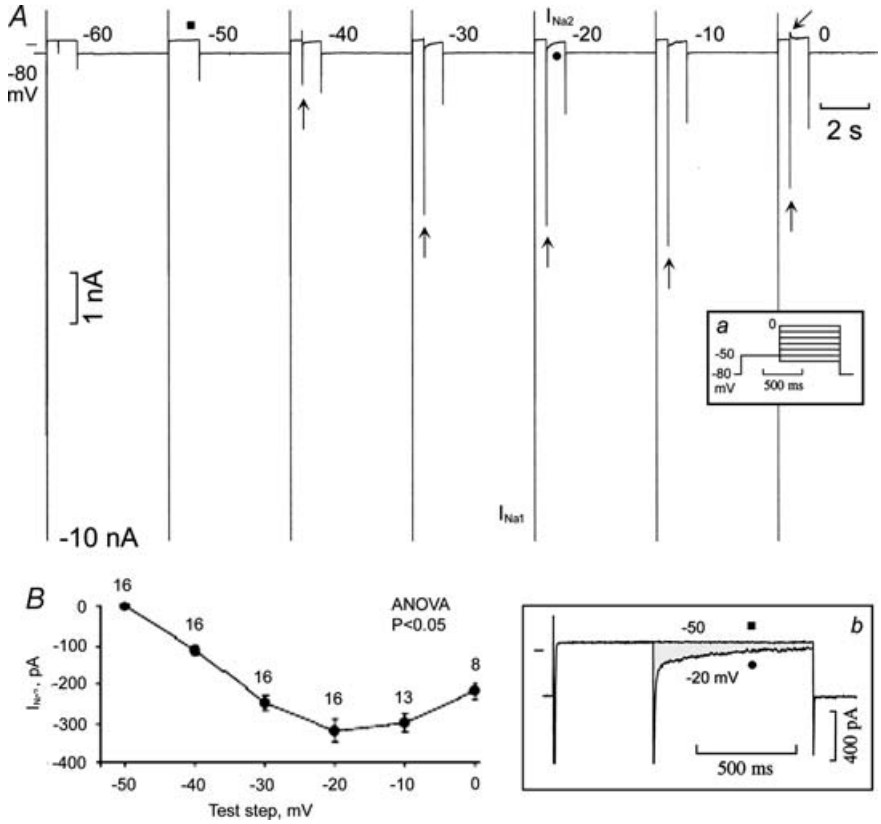

Figure 1. Separation of I_{Na2} from I_{Na1}
The two-step protocol is illustrated in inset *a*. In *A*, the upward arrows point to the fast inward transient that precedes the slowly decaying component of I_{Na2}. The leftward oblique arrow points to the beginning of I_{to}. The traces labelled by ■ and ● are superimposed in inset *b*, in which the shaded area emphasizes the decaying I_{Na2}. In *B*, the graph shows the amplitude of the inactivating component of I_{Na2} during the second steps at the potentials indicated.

upward arrow), which slowly declined as a function of time.

The amplitude of initial fast inward transient increased at −30 mV, reached a peak at −10 mV and then began to decrease (upward arrows). At the same time, the slowly inactivating component of I_{Na2} increased during the step to −30 mV, peaked at −20 mV, and then gradually decreased with larger depolarizations. At 0 mV, the transient outward current, I_{to}, became apparent (oblique arrow) and partly masked I_{Na2}. In inset *b*, the I_{Na2} trace during the −20 mV step (●) was superimposed at higher gain on the current trace recorded during the step to −50 mV (■). The shaded area emphasizes the fast activation and slow inactivation of I_{Na2} with respect to the steady current at −50 mV.

Thus, I_{Na1} appeared at −50 mV in the absence of I_{Na2}. Instead (after the inactivation of I_{Na1}), I_{Na2} appeared at −40 mV or less negative values, activated quickly, decayed slowly, was maximal at −20 mV and was partly masked by the appearance of I_{to} beginning at −10 mV.

In Fig. 2*B* ($n = 16$ tests), the amplitude of the slowly decaying component of I_{Na2} at −40, −30, −20, −10 and 0 mV was −111, −243, −317, −296 and −217 pA, respectively ($P < 0.05$, ANOVA). As indicated in the graph, the number of tests at the two less negative values was smaller owing to the appearance of I_{to}, which did not allow the measurement of I_{Na2} in every test. In the same 16 cells, with one step protocol (500 ms steps from V_h −80 mV to −20 mV), the magnitude of decaying I_{Na2} at −20 mV was of −939 ± 226 pA (+196%, $P < 0.05$ with respect to I_{Na2} separated by means of the two steps protocol).

In $n = 11$ tests, at −20 mV, I_{Na2} activated at a rate of 80 ± 10 pA ms^{-1} ($P < 0.05$) to reach an amplitude of −426 ± 61 pA ($P < 0.05$). Therefore, I_{Na2} had a slower activation rate, was much smaller, occurred at less negative

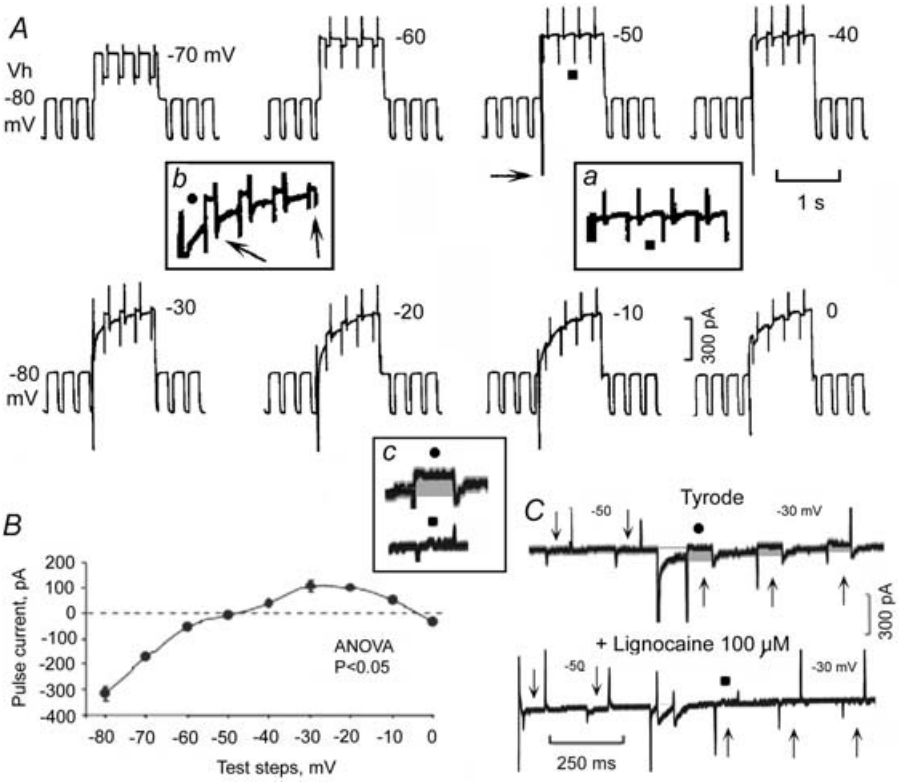

Figure 2. Changes in slope conductance during I_{Na2} in the absence and presence of lignocaine
In *A*, depolarizing steps were applied from V_h −80 mV to the voltages indicated next to the traces. Small (5 mV) and short (80 ms) hyperpolarizing pulses were superimposed at a rate of 240 min^{-1} on the parent steps. The horizontal arrow points to I_{Na1} (only partly shown). Pulse currents are shown at higher gain during the steps at −50 mV (inset *a*) and at −30 mV (inset *b*). The same symbol indicates the same trace within and without the insets. In inset *b*, the arrows point to the difference in amplitude between the first and the last pulse currents. *B* shows the changes in magnitude and polarity of the first pulse current during the parent test steps at the potentials indicated on the abscissa. In *C*, the top trace shows the pulse currents (shaded areas) in Tyrode solution and the bottom trace the currents with the same procedure in the presence of 100 μM lignocaine. The downward and upward arrows point to the current recorded during the superimposed pulses. The traces labelled with ● and ■ are shown at higher gain and temporally aligned in inset *c*.

potentials and inactivated more slowly with respect to I_{Na1}.

In additional experiments, the depolarizing steps were incremented by 1–2 mV in order to determine the threshold potential for the slowly inactivating sodium current in the pacemaker range (I_{Na3}) (Rota & Vassalle, 2003*a*) and I_{Na1} (one step) and that for I_{Na2} (double step). The threshold for I_{Na3} was −58.4 mV ($n = 5$), for I_{Na1} −53.6 mV and for I_{Na3} −44.3 mV ($n = 6$). The maximal amplitude of I_{Na3} was -387 ± 97 pA and that of I_{Na2} with the one-step protocol -989 ± 185 pA. The larger time constant of inactivation (τ_2) of I_{Na3} was 50 ms and that of I_{Na2} was 318 ms (+536%, two-step protocol). The I_{Na3} behaves like a Na^+ current and it is eliminated by TTX and lignocaine (Rota & Vassalle, 2003*a*). Thus, I_{Na1}, I_{Na2} and I_{Na3} were activated singly over different voltage ranges. The inactivation of I_{Na2} and I_{Na3} was slow, I_{Na2} inactivation being much slower than that of I_{Na3}.

Time constant of I_{Na2} inactivation

In $n = 12$ tests, with 800 ms steps at either −30 or −20 mV (maximal I_{Na2}), the time constants of inactivation were τ_1 32 ± 3 ms and τ_2 415 ± 44 ms. Therefore, the decay of I_{Na2} was slow enough and occurred in a suitable potential range (positive to −40 mV) to affect the duration of the plateau in Purkinje fibres, since the duration of the AP is 529.7 ± 28 ms (Lin & Vassalle, 1978) and the plateau is comprised between ∼0 and approximately −30 mV (Draper & Weidmann, 1951).

In $n = 7$ tests, at −20 mV there were no statistical difference in τ_1 and τ_2 in the absence and presence of 0.5 mM 4-aminopyridine (4-AP), suggesting that there is little overlap by I_{to} at the potential at which the time constants of inactivation of maximal I_{Na2} were measured.

Slope conductance following I_{Na1} and during I_{Na2} in the absence and presence of lignocaine

After the quick inactivation of I_{Na1} at −50 mV, the conductance should reflect the inward rectification of the background potassium current (I_{K1}) (Hutter & Noble, 1960; Hall *et al.* 1963) and therefore it would be expected to be small and not varying as a function of time. Instead, I_{Na2} ought to be associated with an initial increase in slope conductance (related to its activation) followed by a decrease as a function of time (related to its inactivation).

As shown in Fig. 2*A*, the slope conductance was measured by superimposing short hyperpolarizing pulses on gradually larger depolarizing parent steps. With depolarizing steps to −70, −60 and −50 mV, the pulse current markedly decreased in amplitude, as expected from I_{K1} inward rectification. At −50 mV, I_{Na1} appeared (only partly shown, horizontal arrow) and, after its quick inactivation, the slope conductance did not change with time (inset *a*).

During the steps at −40, −30 and −20 mV, the pulse current amplitude was larger than at −50 mV, owing to the activation of I_{Na2}, and its polarity was reversed, owing to the negative slope (Gintant *et al.* 1984; Vassalle *et al.* 2007) of the current–voltage relation. As I_{Na2} inactivated, the slope conductance decreased as function of time (at −30 mV, the last pulse current was 72% smaller than the first one; see arrows in inset *b*). The pulse current amplitude was maximal at −30 mV and minimal at −10 mV. The pulse currents re-increased in magnitude and once more became negative at 0 mV, suggesting the activation of a superimposed I_{to}.

In $n = 5$ tests, during the step to −50 mV the pulse current was minimal and did not vary as a function of time. During a step to -28.0 ± 2.0 mV, the first pulse current was 107.6 ± 7.6 pA and the last 35.4 ± 6.4 pA (−67%, $P < 0.05$). In Fig. 2*B*, the average amplitude and the polarity of the first pulse current were plotted as a function of the voltage steps. It is apparent that over the voltage range of I_{Na2} the slope conductance increased and that the pulse current was outward.

The slope conductance was also studied after separation of I_{Na2} from I_{Na1} by means of the two-step protocol in the absence and presence of lignocaine. In Fig. 2*C* (top trace), during the step to −50 mV, I_{Na1} inactivation was followed by unchanging small pulse currents (downward arrows). During the decay of I_{Na2} at −30 mV, the reversed pulse currents (upward arrows) decreased in amplitude with time. In Fig. 2*C* (bottom trace), 100 μM lignocaine blocked I_{Na2} as well as the associated conductance changes (cf. traces labelled by upward arrows in the top and bottom traces). The traces marked by a dot and a square have been aligned in inset *c* and show the suppression of the pulse current by lignocaine.

In $n = 4$ tests, at −50 mV after I_{Na1} inactivation the conductance was minimal and unchanging. With second steps, during the decay of I_{Na2} the amplitude of the first pulse current was 86.2 ± 17.2 pA and that of the last pulse current was 33.0 ± 7.8 pA (−61%, $P < 0.05$). Therefore, the time-dependent decrease in conductance occurred only when I_{Na2} was present (whether or not I_{Na2} was preceded by I_{Na1}). In $n = 2$ tests, 100 μM lignocaine decreased the amplitude of decaying I_{Na2} by −82% with respect to the control value.

Time-dependence of I_{Na2} inactivation

The time-dependent inactivation of the slowly inactivating component of I_{Na2} was tested by first eliciting I_{Na1} at −50 mV and then I_{Na2} at −30 mV after gradually longer intervals, as shown in Fig. 3*A* by the protocol in inset *a*. As the interval between the beginning of the conditioning step at −50 mV and that of the test step to −30 mV increased in

increments of 100 ms, the amplitude of both the fast and of the slowly inactivating components of I_{Na2} gradually decreased (see traces at higher gain in inset *b*).

As shown in Fig. 3*B*, $n = 10$ tests, when the duration of conditioning steps at −50 mV was increased in increments of 100 ms, the amplitude of the slowly decaying I_{Na2} component decreased progressively from −382 pA after 200 ms to −146 pA after 900 ms (−61%, $P < 0.05$ ANOVA). The data of the time-dependent inactivation were fitted by a single exponential function with a time constant of 351.8 ms.

In $n = 4$ tests, no statistical differences were found in the amplitude of I_{Na2} at −30 mV in the absence and presence of 0.5 mM 4-AP, suggesting that at that potential there was little or no overlap of I_{Na2} and I_{to}.

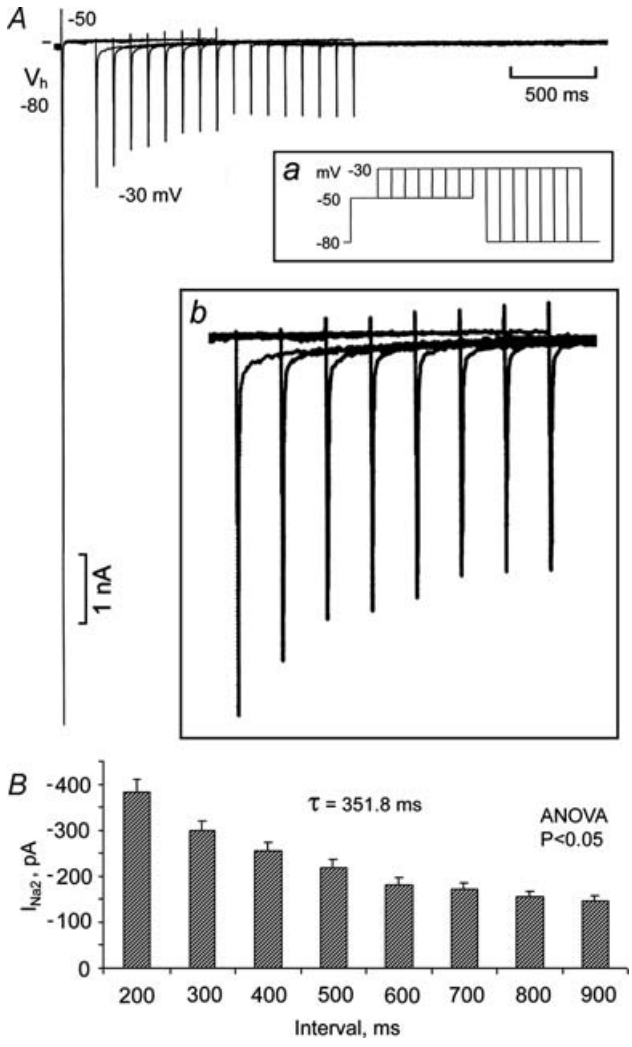

Figure 3. Time-dependent inactivation of I_{Na2} at −50 mV
The protocol is shown in inset *a*. The V_h was −80 mV, and a step to −50 mV was applied for 200 ms with successive increments of 100 ms up to 900 ms. The potential was then clamped to −30 mV for 800 ms and then again to V_h −80 mV. The I_{Na2} traces displayed in *A* are shown at higher gain in inset *b*. The average magnitudes of the decaying I_{Na2} after gradually longer intervals at −50 mV are shown in the graph of *B*. The time constant of the progressive inactivation of I_{Na2} is indicated by τ.

Time-dependent recovery from inactivation of I_{Na2}

If the recovery from inactivation of I_{Na2} is also slow, the plateau duration might decrease at faster rate of discharge, owing to the shorter diastole and a smaller recovery from inactivation of I_{Na2}.

In Fig. 4*A* (protocol in inset *a*), the time-dependent recovery from steady-state inactivation of I_{Na2} was tested by applying hyperpolarizing steps from a V_h of −30 mV to −100 mV for progressively longer periods of time. On return to −30 mV, I_{Na1} was followed by the slowly decaying I_{Na2} (horizontal arrow in Fig. 4*A*). As seen at

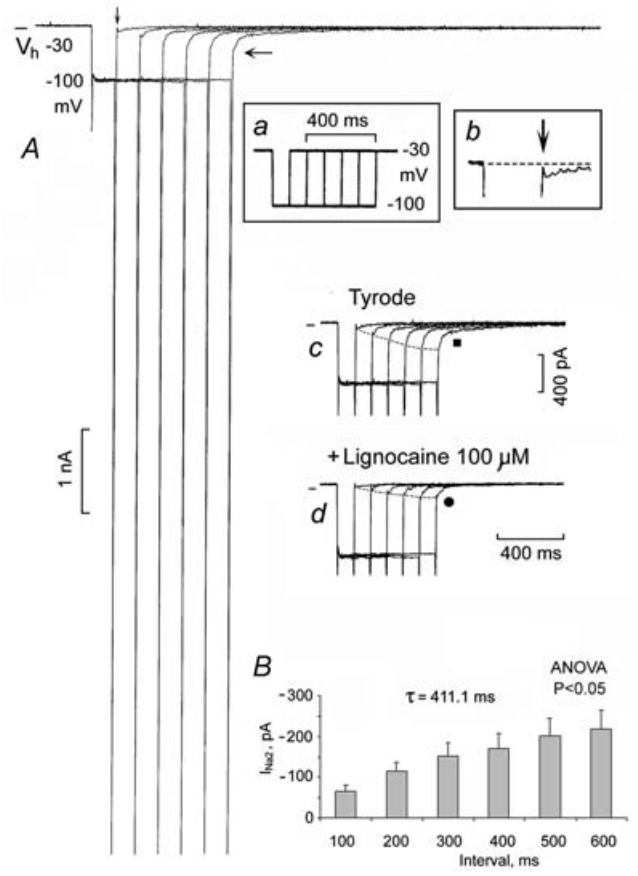

Figure 4. Recovery from inactivation of I_{Na2} as a function of time in the absence and presence of lignocaine
Hyperpolarizing steps were applied from a V_h of −30 mV to −100 mV for progressively longer periods of time (voltage protocol in inset *a*). After the first hyperpolarizing step, the vertical arrow indicates the nearly complete inactivation of I_{Na1} and subsequent activation of a small I_{Na2} (inset *b*). The current traces in the absence (Tyrode) and in the presence of lignocaine (100 μM) are shown as labelled. The dashed lines join the beginning of slowly inactivating I_{Na2} after the steps of increasing duration. In *B*, the graph shows the amplitude of the decaying I_{Na2} as a function of the duration of the hyperpolarizing steps. The time constant of the gradual recovery from inactivation is indicated by τ.

higher gain in inset *b*, after the first 100 ms hyperpolarizing step, a very small I_{Na2} peaked and decayed after the nearly complete inactivation of I_{Na1} (downward vertical arrow). After gradually longer steps, the decaying I_{Na2} started sooner during the inactivation of I_{Na1}, became larger (as emphasized by the dashed line across the traces in inset *c*) and decayed with a larger τ_2. The I_{Na2} recovering from inactivation in Tyrode solution (inset *c*) was reduced by ~40% by 100 μM lignocaine (inset *d*).

The mean values ($n = 5$ tests) of the decaying I_{Na2} on return to −30 mV after repolarization from V_h −30 mV to −100 mV for 100–600 ms are shown in Fig. 4*B* ($P < 0.05$ ANOVA). With respect to the first value, the percentage change in I_{Na2} was +81, +143, +171, +221 and +249%, respectively. The data of the time-dependent recovery from inactivation of I_{Na2} were fitted with a single exponential function with a time constant of 411 ms. Therefore, not only inactivation but also the recovery from inactivation of I_{Na2} is much longer than that of I_{Na1}.

Voltage dependence of I_{Na2} recovery from inactivation

The voltage dependence of recovery from steady-state inactivation of I_{Na2} was studied by applying the protocol shown in inset *a* in Fig. 5.

In Fig. 5*A*, the current traces are superimposed and the oblique arrow points to the slowly inactivating I_{Na2} that followed I_{Na1} after the conditioning steps. In Fig. 5*B*, the single traces are shown. After the −40 mV step, on return to −30 mV neither I_{Na1} nor I_{Na2} were present. After the −50 mV step, I_{Na1} was small (horizontal arrow) and the decaying I_{Na2} was still absent. After the −60 mV step, I_{Na1} (horizontal arrow) was greater than after the previous step and a very small I_{Na2} appeared (shaded area). After the −70, −80 and −90 mV steps, I_{Na2} kept on increasing and inactivated with larger time constants. In Fig. 5*C* ($n = 5$ tests), the average data show that the inactivating I_{Na2} was absent after the steps at −40 and −50 mV and increased slowly and gradually after the more negative steps.

The results suggest that I_{Na2} recovery from inactivation begins with repolarization at −60 mV and increases gradually at more negative potentials.

Voltage-dependent deactivation

As exemplified in Figs 1, 2 and 3, sudden repolarization at the end of I_{Na2} did not elicit an inward tail, suggesting that I_{Na2} quickly deactivated on repolarization to the resting potential (see Carmeliet, 1987), consistent with the sudden restoration of the resting conductance (Fig. 2).

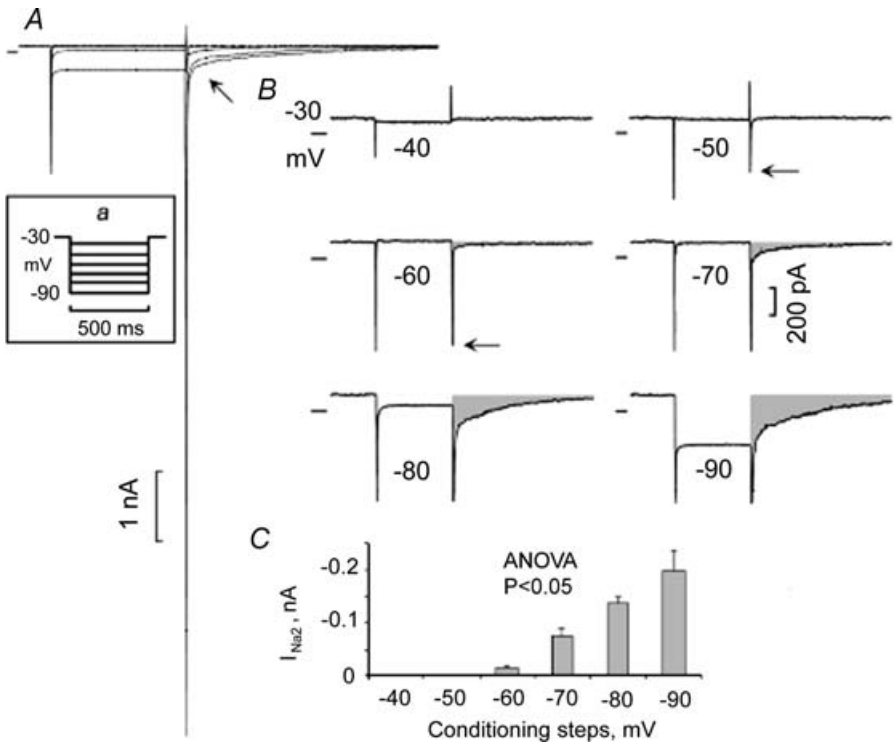

Figure 5. Voltage-dependent recovery of I_{Na2} from inactivation
The protocol is shown inset *a*. The superimposed current traces are shown in *A*. The oblique arrow points to the slowly inactivating I_{Na2} traces that followed the hyperpolarizing steps. The single current traces are shown in *B*, where the shaded areas emphasize the current after the step to the voltage indicated next to the traces. The average magnitude of I_{Na2} (ordinate) after the conditioning steps to different potentials (abscissa) is shown in *C*.

However, the potential at which I_{Na2} starts deactivating has not been determined. The region of negative slope in the current–voltage relation during depolarizing ramps is mostly due to gradual activation and slow inactivation of I_{Na2}, since the negative slope is markedly reduced by TTX, by less negative V_h or by slower ramps (Gintant *et al.* 1984; Vassalle *et al.* 2007). If I_{Na2} deactivation occurs in that potential range, hyperpolarization would suddenly remove the negative slope current. To investigate this point, a slow ramp (60 mV over 400 ms) was applied from V_h −80 mV to −20 mV to induce the region of negative slope in the absence of I_{Na1}. At the end of the ramp, depolarizing steps were applied in increments of 2.5 mV to −10 mV to verify the activation and inactivation of I_{Na2} and hyperpolarizing steps to −37.5 mV to investigate whether and how much I_{Na2} deactivated as a function of repolarization in that range of potentials (protocol in Fig. 6*A*).

In Fig. 6*B*, during the ramp, when the voltage attained the value of −45 mV a region of negative slope appeared. At the end of the ramp, the sudden depolarization from −20 to −10 mV elicited an inward transient which slowly declined, as typical for I_{Na2}. On repolarization to −80 mV, I_{Na2} suddenly deactivated.

In Fig. 6*C*, at the end of the ramp, repolarization from −20 to −37.5 mV shifted the current in an outward direction to a value close to that at the beginning of the negative slope, since apparently the sudden deactivation of I_{Na2} abolished the negative slope current. The trace recorded at −10 mV is superimposed on that at −37.5 mV and the shaded area emphasizes the different effects of depolarization and hyperpolarization from −20 mV.

Therefore, the repolarization to −37.5 mV led to the immediate deactivation of I_{Na2} that had been activated by the depolarizing ramp, thereby abolishing the negative slope current. The superimposed traces in Fig. 6*D* show the gradual changes with the steps applied according to the protocol. The current began to become suddenly outward with the repolarizing steps at −27.5 mV, gradually becoming more outward with repolarizations to −37.5 mV.

In $n = 6$ tests, the negative slope current (measured as the difference between beginning and end of the negative slope region) was −329 ± 89 pA. During the depolarizing step to −10 mV, the amplitude of I_{Na2} was −203 ± 53 pA. During the repolarizing step to −37.5 mV, the current shifted in an outward direction and its amplitude was 190 ± 41 pA (n.s. with respect to the negative slope current).

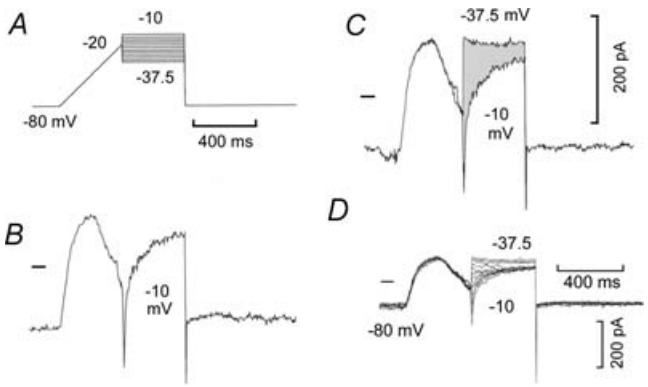

Figure 6. Deactivation of I_{Na2} on repolarization
The protocol included a ramp from V_h −80 to −20 mV and steps to potentials varying from −10 to −37.5 mV in increments of 2.5 mV followed by a return to V_h −80 mV (protocol in *A*). The current traces shown in *B* and *C* were recorded at the potentials indicated next to the traces. The shaded area emphasizes the difference between the currents recorded at the potentials indicated. The superimposed traces recorded with protocol *A* are shown in *D*.

Effects of low $[Na^+]_o$ on I_{Na2}

The dependence of I_{Na2} on $[Na^+]_o$ was studied in a low-sodium solution. In Fig. 7*A*, in Tyrode solution the step to −50 mV elicited I_{Na1}, not followed by a time-dependent current, as usual. The step from −50 to −20 mV elicited a smaller fast activating inward transient (horizontal arrow) followed by the slow inactivation of I_{Na2} (indicated by the shaded area). In Fig. 7*B*, low $[Na^+]_o$ (80.4 mM, −42.5%, substituted with isotonic sucrose) decreased the fast inward transients on depolarization to −50 and −20 mV (horizontal arrow) as well as the inactivating I_{Na2}. In inset *a*, the marked decrease of the decaying I_{Na2} in low $[Na^+]_o$ with respect to control values is emphasized by the shaded areas.

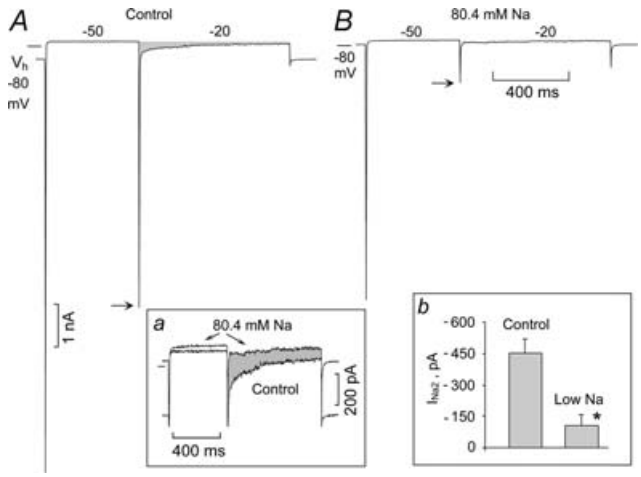

Figure 7. Reduction of I_{Na2} by low $[Na^+]_o$
A 500 ms step from V_h −80 mV to −50 mV was followed by an 800 ms step to −20 mV in control (*A*) and in a low-sodium solution (80.4 mM; *B*). In inset *a*, the traces recorded in control solution and in the presence of low $[Na^+]_o$ are superimposed, the shaded area emphasizing the reduction of I_{Na2} by the low-sodium solution. The average reduction in I_{Na2} in the low-sodium solution is shown in inset *b*. $^*P < 0.05$.

In $n = 5$ tests, at −20 mV the decaying I_{Na2} decreased by −76% ($^*P < 0.05$) in the low-sodium solution, as shown in inset *b*.

Effects of low and high $[Ca^{2+}]_o$ on I_{Na2}

At less negative voltages, an inward movement of calcium could occur during I_{Na2}. If so, I_{Na2} should be modified by substantial changes in $[Ca^{2+}]_o$.

In Fig. 8, depolarizing steps were applied from a V_h of −90 mV to +30 mV in increments of 10 mV (see abscissa in Fig. 8*C*). In Tyrode solution (control, Fig. 8*A*), I_{Na1} appeared at −50 mV (rightward oblique arrow) and I_{Na2} at −40 mV (leftward oblique arrow), as usual. In low $[Ca^{2+}]_o$ (Fig. 8*B*), I_{Na1} appeared at −60 mV and I_{Na2} at −50 mV (arrows). In high $[Ca^{2+}]_o$ (Fig. 8*C*), I_{Na1} appeared at −40 mV and I_{Na2} at −30 mV (arrows). Thus, in low $[Ca^{2+}]_o$, the threshold for both I_{Na1} and I_{Na2} shifted in a negative direction and in high $[Ca^{2+}]_o$ in a positive direction (see Weidmann, 1955). The amplified traces recorded at the threshold for I_{Na2} (leftward oblique arrows) show that there was little difference in this current in the different $[Ca^{2+}]_o$.

The maximal I_{Na2} in the different solutions (labelled by ●, ■ and ★ and shown at higher gain in inset *a*) was also little affected the by low or high $[Ca^{2+}]_o$. In inset *b*, the same I_{Na2} traces in the three solutions were superimposed by the current at the end of the steps and also show little effect of $[Ca^{2+}]_o$ on the amplitude or time course of I_{Na2}. These findings suggest little contribution of calcium to I_{Na2} in the range between −40 and −20 mV.

As shown in Table 1, with the one-step protocol, in low $[Ca^{2+}]_o$ I_{Na2} was not significantly smaller either at the same potential as control traces or at the more negative potential where it was largest. In high $[Ca^{2+}]_o$, I_{Na2} was significantly smaller than the control value at the same potential, but not at the less negative potential where it was maximal. Similar results were obtained with the two-step protocol ($n = 5$ tests).

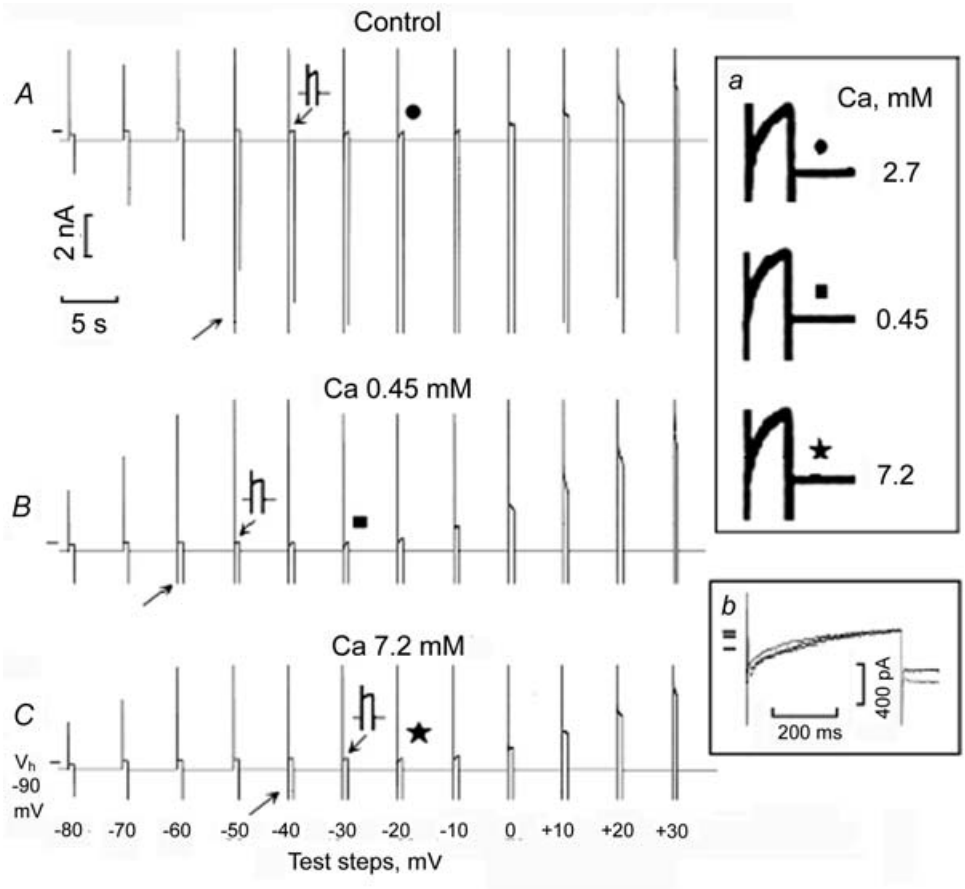

Figure 8. I_{Na2} is little affected by $[Ca^{2+}]_o$ at negative potentials
Depolarizing steps were applied from V_h −90 mV to +30 mV in increments of 10 mV (abscissa) in Tyrode solution (*A*), in 0.45 mM $[Ca^{2+}]_o$ (*B*) and in 7.2 mM $[Ca^{2+}]_o$ (*C*). The rightward oblique arrows point to the threshold for I_{Na1} and the leftward oblique arrows join the traces at high gain to those at normal gain at the I_{Na2} threshold. The traces labelled by ●, ■ and ★ are shown at greater gain in inset *a*, the same symbol identifying the same trace within and without the inset. The same traces are shown superimposed with a faster time base in inset *b*.

Table 1. I_{Na2} in Tyrode solution, in low and in high $[Ca^{2+}]_o$

	V_t (mV)	I_{Na2} (pA)	I_{Na2} (pA)	V_t $I_{Na2,max}$ (mV)	$I_{Na2,max}$ (pA)
Tyrode solution, $[Ca^{2+}]_o$ 0.45 mM ($n = 6$)	-23.3 ± 2.1	-619 ± 73	-527 ± 61 (n.s.)	-28.5 ± 2.1	-589 ± 52 (n.s.)
Tyrode solution, $[Ca^{2+}]_o$ 7.2 mM ($n = 6$)	-25.0 ± 2.2	-686 ± 144	-193 ± 46*	-11.7 ± 3.1	-524 ± 105 (n.s.)

Slowly inactivating component of I_{Na2} in Tyrode solution and in low and high $[Ca^{2+}]_o$ at the same test potential (first three columns) and at the potentials where I_{Na2} was maximal in the two $[Ca^{2+}]_o$ solutions (last two columns). The results were obtained with the one-step protocol. Key: V_t, test step voltage; I_{Na2}, amplitude of the slowly decaying I_{Na2} at the test voltage in Tyrode solution and in the different $[Ca^{2+}]_o$ solutions (first three columns); V_t, $I_{Na2,max}$, voltage test step at which I_{Na2} was largest in low or high $[Ca^{2+}]_o$ (fourth column); $I_{Na2,max}$, amplitude of the maximal I_{Na2} (fifth column) at the voltage indicated in the fourth column; $[Ca^{2+}]_o$ 0.45 mM, results obtained in low $[Ca^{2+}]_o$; and $[Ca^{2+}]_o$ 7.2 mM, results obtained in high $[Ca^{2+}]_o$. *$P < 0.05$.

Effects of 4-aminopyridine and the separation of I_{Na2} from I_{to}

The transient outward current, I_{to}, became apparent beginning with steps to about −10 mV and progressively increased at more positive potentials, masking I_{Na2} and I_{Ca}.

In a first approach, V_h was set at −50 mV, which would largely inactivate the Na^+ currents (see Fig. 5) but not I_{Ca} (Isenberg & Klöckner, 1982). In control conditions (Fig. 9*A*), steps from −50 to +70 mV induced at negative potentials only a small inward transient which inactivated relatively quickly and at positive potentials a progressively larger I_{to}. In the presence of 4-AP (Fig. 9*B*), I_{to} was suppressed. At −20 mV, the small inward transient which inactivated quickly in control conditions was little affected by 4-AP. This suggests that at that potential where I_{Na2} was usually maximal, there was a little contribution of I_{to} and of I_{Ca}. A small contribution of I_{Ca} is consistent with a threshold of −35 mV and with its small time constants of inactivation (at 0 mV, I_{Ca} inactivates with a τ_1 of 6 ms and τ_2 of 30 ms; Isenberg & Klöckner, 1982).

Instead, at +20 mV the elimination of I_{to} by 4-AP unmasked an inward transient (−986 pA) that decayed with a τ_2 of 88 ms (the time constant of I_{Ca} inactivation increases at positive potentials; Isenberg & Klöckner, 1982) but this value was still much smaller than for I_{Na2}. The reversal potential of the inward transient was positive to +70 mV, since at that potential there was still an initial small inward component.

The two-step protocol was applied to verify how the block of I_{to} by 4-AP would affect I_{Na2} at different voltages (not shown). In $n = 7$ tests, during the step to -18.6 ± 2.6 mV, the amplitude of I_{Na2} was -413 ± 112 pA in Tyrode solution and -341 ± 86 pA (n.s.) in the presence of 0.5 mM 4-AP. In the presence of 4-AP, the maximal I_{Na2} shifted to −10 mV (-513 ± 99 nA, $P < 0.05$, with respect to the value in Tyrode solution). These results suggest that there was little or no overlap between I_{Na2} and I_{to} at approximately −20 mV, but also that at −10 mV the incipient activation of I_{to} decreases the apparent amplitude of I_{Na2}. In $n = 10$ tests with the two-step protocol, in the presence of 0.5 mM 4-AP, the reversal potential was $+66.1 \pm 2.3$ mV.

Since I_{Na2} peaks at approximately −20 mV whereas I_{Ca} peaks at more positive values, the amplitude of the time-dependent currents was measured at two different voltages in the presence of 0.5 mM 4-AP. In $n = 13$ tests, the time-dependent current was -396 ± 63 pA at −20 mV and -667 ± 87 pA ($P < 0.05$) at +20 mV. This result suggests a substantial contribution of I_{Ca} at positive potentials.

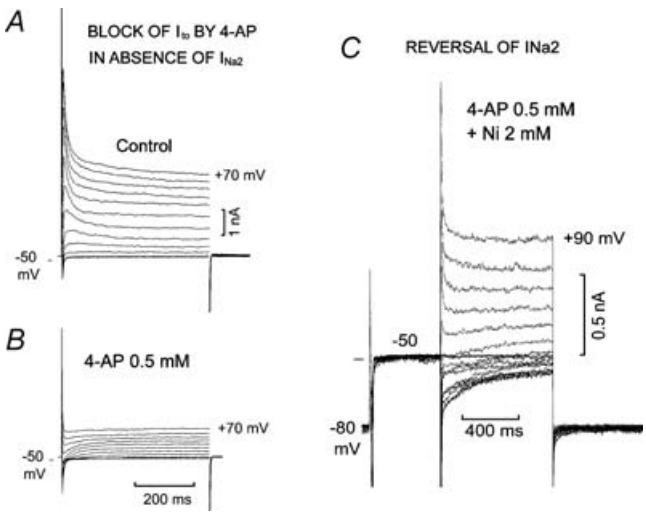

Figure 9. I_{Na2} in the absence and presence of I_{to} block by 4-aminopyridine
In *A* and *B*, V_h was set at −50 mV, and 500 ms depolarizing steps were applied in increments of 10 mV to +70 mV in the absence (*A*) and in the presence (*B*) of 0.5 mM 4-aminopyridine. The reversal of I_{Na2} is shown in *C* in the presence of 0.5 mM 4-AP and of 2 mM Ni^{2+}. The V_h was −80 mV, and 500 ms steps to −50 mV were followed by 800 ms steps to +90 mV in increments of 10 mV.

Reversal potential of I_{Na2}

The two-step protocol was applied also in the presence of both 4-AP (0.5 mM) and nickel (2 mM) in order to suppress I_{to} and I_{Ca}, respectively. In Fig. 9*C*, the first step elicited I_{Na1}, but not consistently. This was possibly due to the presence of Ni^{2+}, which shifts the threshold for I_{Na1} in a positive direction (Hanck & Sheets, 1992). With gradually larger subsequent steps, the decaying I_{Na2} became smaller and reversed close to −60 mV.

In $n = 5$ tests, in Tyrode solution, the threshold for I_{Na1} was -50 ± 0 mV and that for I_{Na2} was -40 ± 0 mV. The I_{Na2} was maximal (-257 ± 39 pA) at a potential of -22.0 ± 2.0 mV and inactivated with a τ_1 of 18 ± 3 ms and a τ_2 of 351 ± 25 ms. In the same cells, in the presence of 0.5 mM 4-AP and 2 mM Ni^{2+}, the threshold for I_{Na1} shifted to -40 ± 4.4 mV and that for I_{Na2} to -26 ± 2.4 mV ($P < 0.05$). The I_{Na2} was maximal (-434 ± 89 pA) at a potential of -10 ± 0 mV ($P < 0.05$) and inactivated with a τ_1 of 13 ± 4 ms and a τ_2 of 384 ± 71 ms. The reversal potential was +60 mV in four cells and there was still a residual I_{to} at large positive potentials in the fifth cell. It should be added that the accuracy of the determination of the I_{Na2} reversal potential might have been affected by contamination with K^+ in both the pipette and the bath solution. The positive shift of the I_{Na2} threshold and of the potential at which I_{Na2} was maximal might have been affected by the presence of Ni^{2+}. The increase in the amplitude of I_{Na2} at -10 mV presumably was also related to the suppression of I_{to} at that potential.

Thus, after the block of I_{to} and I_{Ca}, the slowly inactivating I_{Na2} decreased gradually at more positive potentials where it decayed more slowly and reversed near the value of the Nernst potential for sodium.

Discussion

The results obtained show, for the first time, that in Purkinje cells I_{Na2} is a rapidly activating, slowly inactivating Na^+ current flowing through a channel that has a threshold, voltage dependence, conductance changes, kinetics of inactivation and of recovery from inactivation which are markedly different from those of I_{Na1}. Furthermore, I_{Na2} can be present in the absence of I_{Na1} and vice versa. The voltage range and kinetic properties suggest that I_{Na2} may be important in regulating the action potential duration of Purkinje fibres under normal conditions, such as prevention of re-entry of excitation from the myocardial fibres (Myerburg *et al.* 1970) or the shortening of action potentials with faster rates of discharge (Vassalle & Bocchi, 2007). The I_{Na2} may affect the plateau also under abnormal conditions, such as low resting potential, early after-depolarizations and during the therapeutic administration of sodium channel blockers.

Fast inactivation of I_{Na1} and slow inactivation of I_{Na2}

The different threshold for the appearance of I_{Na1} (-54 mV) and of I_{Na2} (-44 mV), the activation of one current in the absence of the other, their different kinetics of inactivation and recovery from inactivation suggest that two different sodium channel isoforms might be involved in generating I_{Na1} and I_{Na2}.

After the quick inactivation of the I_{Na1} channels at -50 mV, during the steps at less negative values the I_{Na2} channels activated quickly and inactivated far more slowly. Also, at voltages positive to -40 mV, the amplitude of slowly inactivating I_{Na2} increased gradually to a peak (Fig. 1*B*), as does the TTX difference current (Vassalle *et al.* 2007). The increase appears to reflect the activation of additional I_{Na2} channels at those less negative potentials, since the slope conductance increased whereas the driving force decreased.

The two-step procedure yielded a number of other results. It showed that I_{Na2} activation is relatively fast (but not as fast as that of I_{Na1}) and that its slowly inactivating component is small compared with I_{Na1}. The two-step protocol permitted us to rule out that any loss of voltage control during I_{Na1} activation might affect I_{Na2} recording. Thus, by the time the inactivation of I_{Na1} was completed, the current was indistinguishable from that recorded at -60 mV in the absence of I_{Na1}. This is further supported by the fact that the slope conductance reached a minimum at -50 mV (owing to the inward rectification of I_{K1}; Hutter & Noble, 1960; Hall *et al.* 1963) and did not change with time during the step (Fig. 2). Furthermore, the two-step protocol quantified the decrease in I_{Na2} to be expected with the shift of the potential from a V_h of -80 mV to -50 mV and allowed the determination of the gradual inactivation of I_{Na2} in the absence of I_{Na1} (Fig. 3).

While it cannot be excluded that in some tests a small residual I_{Na1} might have contributed to the I_{Na2} fast inward transient, I_{Na1} (due to its fast inactivation) would not affect the magnitude of slowly inactivating I_{Na2}. The importance of this point is related to the fact that only the slowly inactivating I_{Na2} would influence the duration of the plateau (whereas the fast activation of I_{Na2} would contribute to the upstroke of the action potential). The conclusion that I_{Na2} is related to a Na^+ channel isoform different from that of I_{Na1} seems also indicated by the finding that during depolarizing ramps the negative slope current is present even in the absence of I_{Na1} and a small depolarizing step at the end of the negative slope elicits only I_{Na2} (Fig. 6). Furthermore, I_{Na2} suddenly deactivated on repolarization even at potentials less negative than the resting potential.

In canine Purkinje fibres, TTX shortened the AP at lower (3.3×10^{-8} M) concentrations than those ($\sim 10^{-6}$ M) which decreased the amplitude and maximal rate of rise of the action potential. This shortening was attributed to a current flowing through a background sodium conductance and/or fewer sodium channels that do not inactivate or a different mechanism of inactivation (Coraboeuf *et al.* 1979).

The slow inactivation of I_{Na2} as a function of time and of voltage rules out the possibility that I_{Na2} is due to background sodium channel or to the window current (Attwell *et al.* 1979). The window current would cause

a negative slope region sensitive to TTX (Gintant *et al.* 1984), as does I_{Na2} (Vassalle *et al.* 2007). However, I_{Na2} (in addition to being time dependent) has a voltage range more positive (−40 to +60 mV) than the range (−65 to −15 mV; Attwell *et al.* 1979) of the window current.

In rabbit Purkinje fibres, a slowly inactivating current was suppressed by TTX, Na^+ withdrawal and 0.2 mM Cd^{2+}. The time course of inactivation had different phases with different time constants (from a few hundred milliseconds to tens of seconds at −45 mV). The current–voltage relation extended from −85 to +40 mV, the current peaking at −20 mV and deactivating quickly. It was concluded that Na^+ channels show multiple states of inactivation and that the slowly inactivating Na^+ current plays an important role in determining the diastolic potential, pacemaker activity and plateau duration (Carmeliet, 1987). The differences between the rabbit slowly inactivating current and I_{Na2} may be related to differences in the species used, since, for example, the rabbit Purkinje fibres have little diastolic depolarization (see Carmeliet & Mubagwa, 1986), in contrast to canine Purkinje fibres (Draper & Weidmann, 1951). Some differences may also depend on the methods used (i.e. rabbit Purkinje non-dissociated strands *versus* canine Purkinje single cells used here).

In addition, the slowly inactivating current in Purkinje fibres (Gintant *et al.* 1984; Carmeliet, 1987) might have been a combination of I_{Na2} (Vassalle *et al.* 2007; present results) and I_{Na3} (Rota & Vassalle, 2003*a*). These two TTX-sensitive currents have different activation ranges and can be separated by suitable procedures (Rota & Vassalle, 2004). The I_{Na2} affects the plateau and I_{Na3} the final diastolic depolarization. In agreement with the findings of Carmeliet (1987), I_{Na2} was maximal at approximately −20 mV, recovered relatively slowly and deactivated suddenly. As for the deactivation, the present results show that repolarization to about −25 mV began deactivating I_{Na2}. Repolarization to −37.5 mV removed the negative slope current, which suggests that I_{Na2} is deactivated by the end of the plateau. Therefore, I_{Na2} (whose characteristics we found to be markedly different from those of I_{Na1}) appears to have been a large component of the currents recorded by Gintant *et al.* (1984) and by Carmeliet (1987).

The question should be asked whether I_{Na2} is the same current as the late or persistent sodium current, I_{pNa}, described in ventricular myocardial cells (see Zygmunt *et al.* 2001; Noble & Noble, 2006; Belardinelli *et al.* 2006; Undrovinas *et al.* 2006). Recordings of single sodium channel current show several substantial differences between I_{pNa} and I_{Na2} in that the slow component of inactivation of the former occurred within a more negative range (−60 to −30 mV) and with a much smaller time constant (τ_1 8 and τ_2 14 ms) in rat myocardium. The I_{pNa} channels had the same conductance and reversal potential as the fast Na^+ channels and were blocked by tetrodotoxin, but I_{pNa} was caused by repeated openings of Na^+ channels (Patlak & Ortiz, 1985). In guinea-pig ventricular cells, maximal I_{pNa} was obtained with depolarizing steps from −130 mV to −30 or −20 mV and had a range between −70 and +30 mV (Sakmann *et al.* 2000). However, the plateau of myocardial cells is much more positive than that of Purkinje cells and it is closer to the reversal potential (+33.5 mV) of I_{pNa}. Concerning the sodium channel involved, no definite conclusions were drawn (Sakmann *et al.* 2000). These findings suggest that I_{Na2} in Purkinje cells and I_{pNa} in myocardial cells show similarities, but it seems uncertain whether the same Na^+ channel is involved. Further experimentation is needed to address this question.

Qualitative and quantitative differences between I_{Na2} in Purkinje cells and I_{pNa} in myocardial cells would be expected on the basis of several findings, such as the different voltage range of the plateau in the two tissues and the much longer AP in Purkinje fibres than in myocardial fibres in the same species (approximately +70%; Lin & Vassalle, 1978). Also, in canine tissues, TTX (Coraboeuf *et al.* 1979; Bhattacharyya & Vassalle, 1982), local anaesthetics (Vassalle & Bhattacharyya, 1980), veratridine and $[Na^+]_o$ (Iacono & Vassalle, 1990) modified the myocardial fibre AP much less than that of Purkinje fibres. In addition, little or no I_{Na2} was present in ventricular myocardial cells isolated from the same hearts and studied with the same methods as the Purkinje cells (Bocchi & Vassalle, 2000). Also, TTX decreased the intracellular Na^+ activity far more in Purkinje than in myocardial fibres (Iacono & Vassalle, 1990).

The ion carrying I_{Na2}

Several findings show that I_{Na2} is carried by Na^+ ions. Thus, I_{Na2} was inward, started at a voltage (−44 mV) that does not (Isenberg & Klöckner, 1982) initiate I_{Ca}, was decreased by a less negative V_h (e.g. −50 mV) that does not affect I_{Ca} (Isenberg & Klöckner, 1982), was decreased in a lower $[Na^+]_o$, was little affected by a substantial decrease or increase in $[Ca^{2+}]_o$, was associated with an enhanced conductance that underwent a time-dependent decrease, was not suppressed by nickel or 4-AP, and reversed near the Nernst potential for sodium. Accordingly, I_{Na2} was reduced by TTX but not by manganese (Vassalle *et al.* 2007). By avoiding the systematic use of channel blockers, it was also possible to observe the interactions among different currents that occur in the physiological setting.

The voltage range and kinetics of I_{Na2} and the plateau potential

The voltage range and the large time constant of inactivation make I_{Na2} suitable to influence the plateau

duration in the voltage range which in Purkinje fibres is comprised between ∼0 and roughly −30 mV (Draper & Weidmann, 1951). Beginning at approximately −10 mV, I_{to} appeared, as indicated by a loss of bi-exponential decay and by the increase in the slowly inactivating current in the presence of 4-AP block of I_{to}. With I_{Na2} inactivated by a V_h of −50 mV in the presence of 4-AP, depolarizing steps did not unmask a slowly inactivating I_{Ca} at potentials where I_{Na2} is maximal (−30 to −20 mV).

Once the peak of the upstroke is attained, I_{to} leads to the large and rapid phase 1 repolarization of the Purkinje cell action potential. At the end of phase 1 repolarization, the rapid decay of I_{to} and the slow decay of I_{Na2} would then contribute to set the voltage range and duration of the plateau.

I_{Na2} and sodium channels in the heart

Nine different sodium channel isoforms ($Na_V1.1$ to $Na_V1.9$) have been identified and functionally expressed (Catterall *et al.* 2005). In cardiac tissues, three kinds of sodium channels (cardiac, neuronal and skeletal) are expressed, which have different characteristics (and presumably different functions). The cardiac isoforms ($Na_V1.5$, $Na_V1.8$ and $Na_V1.9$) activate and inactivate quickly and are less sensitive to TTX. Neuronal Na^+ channels ($Na_V1.1$, $Na_V1.2$, $Na_V1.3$, $Na_V1.6$ and $Na_V1.7$) and the skeletal muscle isoform, $Na_V1.4$, inactivate slowly and are more sensitive to tetrodotoxin than the cardiac isoforms.

Therefore, either the neuronal or the skeletal muscle isoforms might be involved in the greater duration of the plateau in cardiac Purkinje fibres. The neuronal $Na_V1.1$, $Na_V1.2$ and $Na_V1.3$ (Haufe *et al.* 2005) and skeletal $Na_V1.4$ isoforms (Qu *et al.* 2007) are expressed in canine Purkinje cells. While such an expression elicits the question of their function in Purkinje cells, further experimentation is needed to determine which sodium channel isoform might underlie I_{Na2}. Furthermore, there is a need to investigate the several different mechanisms that might possibly contribute to the persistent sodium currents (including one or more types of sodium channels, e.g. see Sakmann *et al.* 2000; Zygmunt *et al.* 2001; Undrovinas *et al.* 2006).

As for the processes underlying fast and slow inactivation, they are distinct pharmacologically, kinetically and molecularly. Fast inactivation occurs when an inactivating particle closes the channel pore. Slow inactivation is a different, more complex mechanism that may involve a conformational change of the pore as well as changes in different regions of the channel (for detailed discussion and references see Goldin, 2003 and Ulbricht, 2005). It should be emphasized here that the induction of slow inactivation required prolonged depolarizations, whereas I_{Na2} activates quickly and inactivates slowly with depolarizing steps from the resting potential to −40 mV or less negative values.

In the present context, it is of interest that in cardiac muscle fast inactivation may inhibit slow inactivation, since mutations of fast inactivation modify slow inactivation (Featherstone *et al.* 1996; Richmond *et al.* 1998). This appears to be so for I_{Na3} but not for I_{Na2}. Thus, depolarizing steps in increments of a few millivolts elicit I_{Na3} over a potential range (−60 to −50 mV) negative to I_{Na1} threshold, but when the threshold of I_{Na1} is attained (−50 mV), no I_{Na3} follows I_{Na1} (Rota & Vassalle, 2003*a*; present results). That I_{Na1} might suppress the slow inactivation of I_{Na3} seems to be supported by the fact that, if the threshold for I_{Na1} is shifted to values less negative than −50 mV by decreasing V_h by a few millivolts, the decaying I_{Na3} appears also at −50 mV (Rota & Vassalle, 2003*b*). In contrast, at −40 mV or less negative values, the slow inactivation of I_{Na2} is not suppressed by the fast inactivation of I_{Na1}, since the slow inactivating I_{Na2} follows the latter.

The significance of this behaviour may be related to the different functions of I_{Na2} and I_{Na3}. The I_{Na3} allows diastolic depolarization to attain the threshold for I_{Na1}; once this is accomplished, I_{Na3} would not have further use. In contrast, a suppression of the slow inactivation of I_{Na2} by the fast inactivation of I_{Na1} would wipe out the very function of former (long duration of the plateau).

Conclusions

The different characteristics of I_{Na1}, I_{Na2} and I_{Na3} suggest that different sodium channels may subserve different functions. Thus, in Purkinje fibres the upstroke of the AP would require a regulation different from that of the plateau. If the cardiac rate increases (shorter diastole), neither the amplitude nor the rate of rise of the usptroke ought to decrease, owing to several factors: the fast inactivation and rapid recovery from inactivation of I_{Na1}, the more negative take-off potential due to shorter diastolic depolarization and the hyperpolarization induced by the frequency-dependent increase in the outward current created by the electrogenic Na^+–K^+ pump (Vassalle, 1970). The more negative take-off potential would foster an increased availability of the fast Na^+ channels.

The importance of these factors is that amplitude and rate of rise of the upstroke are essential for a fast conduction velocity (which is the function of ventricular Purkinje fibres under normal conditions). In contrast, if the long AP of Purkinje fibres were not to shorten with faster rates (e.g. at a rate of 120 beats min^{-1} the cycle length would be shorter that the AP), the propagated upstroke might encounter the absolute refractory period, resulting in block of conduction. If the upstroke were to fall in the relative refractory period, a slower conduction would ensue, which might facilitate re-entry of excitation.

Our results suggest a possible sequence of events during the action potential of Purkinje fibres. On depolarization to its threshold, I_{Na2} would activate and contribute to the upstroke and, during the plateau, I_{Na2} would inactivate as a function of time and deactivate as a function of further repolarization. This seems to imply that repolarization of plateau to values more negative than approximately −30 mV would deactivate whatever I_{Na2} is not inactivated. The deactivation of I_{Na2} would accelerate the phase 3 repolarization and during diastole the gradually decaying inactivation would not cause a slowly decaying voltage tail. Such a tail would oppose the diastolic depolarization induced by the slow decay of the pacemaker current, I_{Kdd} (Vassalle *et al.* 1995, 1999; Vassalle, 2007). Instead, during diastolic depolarization, I_{Na2} would start to recover from inactivation and more rapidly so because of the negativity of the diastolic potential. An increase in rate would impinge upon the recovery from inactivation of I_{Na2} by shortening the diastolic interval; hence the shortening of the action potentials (Vassalle & Bocchi, 2007).

As the pacemaker potential enters the voltage range of I_{Na3}, the activation of this current (together with the inward rectification of I_{K1} and the decay of the pacemaker current, I_{Kdd}) would lead to the attainment of I_{Na1} threshold. The rapid inactivation of I_{Na1} would suppress the slow inactivation of I_{Na3} and at less negative potentials I_{Na2} would be brought into play. The cycle would then restart.

References

Attwell D, Cohen I, Eisner D, Ohba M & Ojeda C (1979). The steady state TTX-sensitive ('window') sodium current in cardiac Purkinje fibres. *Pflugers Arch* **379**, 137–142.

Baumgarten CM & Isenberg G (1977). Depletion and accumulation of potassium in the extracellular clefts of cardiac Purkinje fibres during voltage clamp hyperpolarisation and depolarisation. *Pflügers Arch* **386**, 19–31.

Belardinelli L, Shryock JC & Fraser H (2006). Inhibition of the late sodium current as a potential cardioprotective principle: effects of the late sodium current inhibitor ranolazine. *Heart* **92** (Suppl. IV), iv6–iv14.

Bhattacharyya ML & Vassalle M (1982). Effect of tetrodotoxin on electrical and mechanical activity of cardiac Purkinje fibers. *J Electrocardiol* **15**, 351–360.

Bocchi L & Vassalle M (2000). An analysis of the slow sodium current in single Purkinje and myocardial cells. *FASEB J* **14**, A699.

Carmeliet E (1987). Slow inactivation of the sodium current in rabbit cardiac Purkinje fibres. *Pflügers Arch* **408**, 18–26.

Carmeliet E & Mubagwa K (1986). Characterization of the acetylcholine-induced potassium current in rabbit cardiac Purkinje fibres. *J Physiol* **371**, 219–237.

Carmeliet E & Saikawa T (1982). Shortening of the action potential and reduction of the pacemaker activity by lidocaine, quinidine and procainamide in sheep cardiac Purkinje fibers. An effect on Na or K currents? *Circ Res* **50**, 257–272.

Catterall WA, Goldin AL & Waxman SG (2005). International Union of Pharmacology. XLVII. Nomenclature and structure-function relationships of voltage-gated sodium channels. *Pharmacol Rev* **57**, 397–409.

Cohen IS & Kline R (1982). K^+ fluctuations in the extracellular spaces of cardiac muscle. Evidence from the voltage clamp and extracellular K^+-selective microelectrodes. *Circ Res* **50**, 1–16.

Coraboeuf E, Deroubaix E & Coulombe A (1979). Effects of tetrodotoxin on action potentials of the conducting system in the dog heart. *Am J Physiol Heart Circ Physiol* **236**, H561–H567.

Datyner N, Gintant G & Cohen IS (1985). Microprocessor controlled trituration device for the dissociation of cardiac and other tissues. *Pflügers Arch* **403**, 105–108.

Draper MH & Weidmann S (1951). Cardiac resting and action potentials recorded with an intracellular electrode. *J Physiol* **15**, 74–94.

Featherstone DE, Richmond JE & Ruben PC (1996). Interaction between fast and slow inactivation in Skm1 sodium channels. *Biophys J* **71**, 3098, B3109.

Gintant GA, Datyner NB & Cohen IS (1984). Slow inactivation of a tetrodotoxin-sensitive current in canine cardiac Purkinje fibers. *Biophys J* **45**, 509–512.

Goldin AL (2003). Mechanisms of sodium channel inactivation. *Curr Opin Neurobiol* **13**, 284–290.

Hall AE, Hutter OF & Noble D (1963). Current–voltage relations of Purkinje fibres in sodium-deficient solutions. *J Physiol* **166**, 225–240.

Hanck DA & Sheets MF (1992). Extracellular divalent and trivalent cation effects on sodium current kinetics in single canine cardiac Purkinje cells. *J Physiol* **454**, 267–298.

Haufe V, Cordeiro JM, Zimmer T, Wub WS, Schiccitano S, Benndorf K & Dumaine R (2005). Contribution of neuronal sodium channels to the cardiac fast sodium current I_{Na} is greater in dog heart Purkinje fibers than in ventricles. *Cardiovasc Res* **65**, 117–127.

Hutter OF & Noble D (1960). Rectifying properties of cardiac muscle. *Nature* **188**, 495.

Iacono G & Vassalle M (1990). On the mechanism of the different sensitivity of Purkinje and myocardial fibers to strophanthidin. *J Pharmacol Exp Ther* **253**, 1–12.

Isenberg G & Klöckner U (1982). Calcium currents of isolated bovine ventricular myocytes are fast and of large amplitude. *Pflügers Arch* **395**, 30–41.

Lin C-I & Vassalle M (1978). Role of sodium in strophanthidin toxicity of Purkinje fibers. *Am J Physiol Heart Circ Physiol* **234**, H477–H486.

Myerburg RJ, Stewart W & Hoffman BF (1970). Electrophysiological properties of the canine peripheral A-V conducting system. *Circ Res* **26**, 361–378.

Noble D & Noble PJ (2006). Late sodium current in the pathophysiology of cardiovascular disease: consequences of sodium-calcium overload. *Heart* **92** (Suppl. 4), iv1–iv5.

Patlak JB & Ortiz M (1985). Slow currents through single sodium channels of the adult rat heart. *J Gen Physiol* **86**, 89–104.

Qu Y, Karnabi E, Chahine M, Vassalle M & Boutjdir M (2007). Expression of skeletal muscle $Na_V1.4$ Na channel isoform in canine cardiac Purkinje myocytes. *Biochem Biophys Res Commun* **355**, 28–33.

Richmond JE, Featherstone DE, Hartmann HA & Ruben PC (1998). Slow inactivation in human cardiac sodium channels. *Biophys J* **74**, 2945–2952.

Rota M & Vassalle M (2003*a*). Patch-clamp analysis in canine cardiac Purkinje cells of a novel sodium component in the pacemaker range. *J Physiol* **548**, 147–165.

Rota M & Vassalle M (2003*b*). Separation of I_{Na} from the I_{Na3} component in canine cardiac Purkinje cells. *FASEB J* **17**, A116.

Rota M & Vassalle M (2004). Different Na^+ currents in single Purkinje cells. *FASEB J* **18**, A227.

Saint DA, Ju YK & Gage PW (1992). A persistent sodium current in rat ventricular myocytes. *J Physiol* **453**, 219–231.

Sakmann BF, Spindler AJ, Bryant SM, Linz KW & Noble D (2000). Distribution of a persistent sodium current across the ventricular wall in guinea pigs. *Circ Res* **87**, 910–914.

Ulbricht W (2005). Sodium channel inactivation: molecular determinants and modulation. *Physiol Rev* **85**, 1271–1301.

Undrovinas AI, Belardinelli L, Undrovinas NA & Sabbah HN (2006). Ranolazine improves abnormal repolarization and contraction in left ventricular myocytes of dogs with heart failure by inhibiting late sodium current. *J Cardiovasc Electrophysiol* **17**, S169–S177.

Vassalle M (1970). Electrogenic suppression of automaticity in sheep and dog Purkinje fibers. *Circ Res* **27**, 361–377.

Vassalle M (2007). The vicissitudes of the pacemaker current I_{Kdd} of cardiac Purkinje fibers. *J Biomed Sci* **14**, 699–716.

Vassalle M & Bhattacharyya M (1980). Local anesthetics and the role of sodium in the force development by canine ventricular muscle and Purkinje fibers. *Circ Res* **47**, 666–674.

Vassalle M & Bocchi L (2007). Slow sodium current I_{Na2} and frequency changes in Purkinje cells. *FASEB J* **21**, Abstract 956.5.

Vassalle M, Yu H & Cohen IS (1995). The pacemaker current in cardiac Purkinje myocytes. *J Gen Physiol* **106**, 559–578.

Vassalle M, Yu H & Cohen IS (1999). Pacemaker channels and cardiac automaticity. In *Cardiac Electrophysiology. From Cell to Bedside*, ed. Zipes DP & Jalife J, pp. 94–103. W. B. Saunders Co., Philadelphia.

Vassalle M, Bocchi L & Du F (2007). A slowly inactivating sodium current (I_{Na2}) in the plateau range in canine cardiac Purkinje single cells. *Exp Physiol* **92**, 161–173.

Weidmann S (1955). Effects of calcium ions and local anaesthetics on electrical properties of Purkinje fibres. *J Physiol* **129**, 568–582.

Zilberter YI, Starmer CF, Starobin J & Grant AO (1994). Late Na channels in cardiac cells: the physiological role of background Na channels. *Biophys J* **67**, 153–160.

Zygmunt AC, Eddlestone GT, Thomas GP, Nesterenko VV & Antzelevitch C (2001). Larger late sodium conductance in M cells contributes to electrical heterogeneity in canine ventricle. *Am J Physiol Heart Circ Physiol* **281**, H689–H697.

Acknowledgements

This work was supported in part by a grant from National Institutes of Health (HL56092).

Author's present address

L. Bocchi: Dipartimento di Biologia Evolutiva e Funzionale, Sezione Fisiologia, Università di Parma, Viale G. P. Usberti 11/A, Campus Universitario 43100 Parma, Italy.